

Flaky-Shaped Iron Powder “KIP MG150D” for Soft Magnetic Applications*



Naomichi Nakamura
Dr. Eng.,
Senior Researcher,
Iron Powder &
Magnetic Materials
Lab.,
Technical Res. Labs.



Yukiko Ozaki
Dr. Sci.,
Senior Researcher,
Iron Powder &
Magnetic Materials
Lab.,
Technical Res. Labs.



Kazuo Higuchi
Chief Line Manager,
Iron Powder & Weld-
ing Materials Sec.,
Iron Powder & Weld-
ing Materials Dept.,
Chiba Works

Synopsis:

A flaky-shaped reduced iron powder “KIP MG150D” gives an initial permeability at the highest level of iron powder cores. A core with a green density of approximately 90% of the theoretical iron density shows a DC relative initial permeability close to 100, which is about 30% higher than that of a normal reduced powder core through the same compaction process therein no flake shaping is effected. Furthermore, another advantage of the flaky-shaped powder is that the improvement of the initial permeability is attained without deterioration of core loss nor its frequency characteristics. The powder particle planes align along the direction of the magnetic field applied to the core. This lamellar structure is considered to contribute to the improvement of magnetic properties through the reduction of demagnetizing effect and the eddy current loss.

1 Introduction

Magnetic cores produced by compression molding of iron powder have a high saturation magnetic flux density in comparison with sintered ferrites and magnetic alloy powder cores, and also offer a high flexibility in shape design. Based on these advantages, iron powder cores have been applied as line noise filters, smoothing choke coils and similar components.^{1,2)} Among the various types of iron powder, it has been reported that a reduced iron powder gives higher initial permeability than atomized iron powder.^{3,4)}

One requirement for expanding the application of iron powder cores is to improve the initial permeability. Shape modification to produce flat, or “flaky-shaped” iron powder particles is one of the effective ways for this purpose.^{5,6)} To date, efforts have been made to modify an atomized powder to produce flaky-shaped iron powder.⁶⁾ However, very limited studies have been reported on the effect of particle shape modification on the magnetic properties when a reduced iron powder with superior magnetic properties is made flaky-shaped.

This article describes the properties of a flaky-shaped reduced iron powder named KIP MG150D. This iron powder gives a powder core a DC relative initial permeability close to 100, which is the highest level among

iron powder cores. The effects of particle shape modification on the initial permeability and core loss in high frequency region are also discussed.

2 Concept to Improve Permeability of Powder Cores through Particle Shape Modification

First, we review the relationship between particle shape and permeability when the shape of the iron powder particle is approximated as an ellipsoid. When a magnetic field H is applied parallel to the long axis of the ellipsoid, the demagnetization factor N decreases as an ratio of the long axis to short axis increases, namely particle shape becomes more flaky.⁷⁾ By expressing the magnetization in a magnetic field H as M , the effective magnetic field which acts on particles having a demagnetization factor of N is given as $H - NM$. Accordingly, the relative permeability with respect to a single iron powder particle μ/μ_0 can be derived as Eq. (1) by using the relationship $B = \mu H = \mu_0 (M + H)$:

$$\mu/\mu_0 = 1 + (\mu_r - \mu_0) / \{ \mu_0 + (\mu_r - \mu_0) N \} \cdots (1)$$

Where μ_r is the permeability at $N = 0$ and μ_0 is vacuum permeability. Thus, if iron powder particles can be flattened and their particle planes is aligned in the direction

* Originally published in *Kawasaki Steel Giho*, 33(2001)4, 184-187

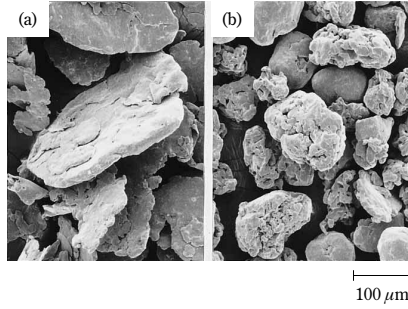


Photo 1 SEM image of the iron powders used: (a) MG150D, (b) MG270H

of the magnetic field, the demagnetization factor N decreases and thereby permeability is enhanced. This is the basic concept on the effect of particle shape modification on permeability of a powder core.

Since an actual powder core is a multi-particle system, a single particle model such as Eq. (1) is not appropriate to estimate permeability, and the interaction between the powder particles should be taken into account. Ollendorf⁶⁾ derived Eq. (2) to express the DC relative initial permeability, μ_{DC}/μ_0 , of powder cores.

$$\mu_{DC}/\mu_0 = \eta (\mu_t - \mu_0) / \{N_{eff} (1 - \eta) (\mu_t - \mu_0) + \mu_0\} \dots (2)$$

Where η and μ_t are the packing fraction, and the intrinsic permeability determined by the material properties of the particles, respectively. N_{eff} is the effective demagnetization factor of the powder core. N_{eff} calculated by Eq. (2) is generally different from N , the demagnetization factor for a single particle which appeared in Eq. (1). Nevertheless, the value of N_{eff} is also reduced by particle shape modification. A more detailed discussion of this point will be presented in Chapter 5.

3 Powder Properties of Test Powders

The flake-shaped iron powder MG150D is produced by grinding a reduced iron powder, followed by screening with a sieve of an opening of $500 \mu\text{m}$. An SEM image of particles of MG150D is shown in **Photo 1**, together with an image of the conventional reduced iron powder KIP MG270H which was not shape-modified. The difference in the particle shape of the two iron powders is clearly observed in these photos. The apparent densities of the test powders MG150D and MG270H were 1.50 and 2.72 Mg/m^3 , respectively. As shown in **Fig. 1**, the particle size distribution of the flake-shaped powder MG150D shows a wider in comparison with that of MG270H.

4 Experimental Procedure

The iron powders were mixed with an epoxy resin (1 mass%) and zinc stearate (0.1 mass%). The epoxy

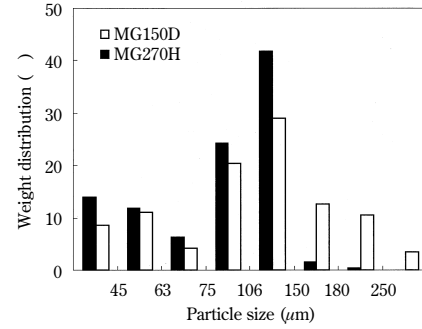


Fig. 1 Particle size distribution of the iron powders used

resin was added for electrical insulation and mechanical binding between the powder particles. The zinc stearate was added as a lubricant. The mixtures were then compacted into a ring shape (outer diameter, 38 mm; inner diameter, 25 mm; thickness, 6.2 mm) at pressures of 490 and 686 MPa. These compacts were heat treated in air for 30 min at 180°C to solidify the epoxy resin. The green density d was calculated from the mass and size of the test piece. The packing fraction η was defined as the ratio of the green density to the true iron density of iron (7.87 Mg/m^3).⁹⁾ The AC initial permeability μ_i was calculated from the measured value of complex impedance obtained by using an LCR meter (Hewlett-Packard, Model 4824A). The measurement frequency range was 10 to 1 000 kHz. Core loss P_{cv} was measured with a BH analyzer (Hewlett-Packard, Model 5060A). The measurement frequency range for P_{cv} was from 1 to 100 kHz, and the measurement magnetic flux density was 50 mT.

5 Results and Discussion

5.1 Initial Permeability

The frequency dependence of the AC relative initial permeability μ_i/μ_0 of powder cores compacted at a pressure of 686 MPa is shown in **Fig. 2**. It is clearly shown that μ_i/μ_0 of the flake-shaped iron powder MG150D is higher than that of with the conventional reduced iron

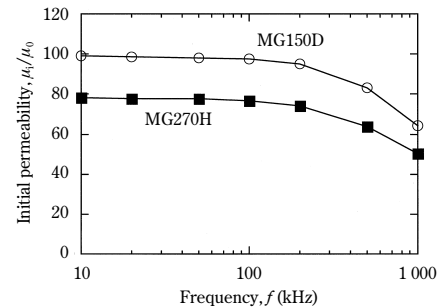


Fig. 2 Frequency dependence of initial permeability for core samples compacted at 686 MPa

Table 1 Characteristics of core samples

	Compaction pressure (MPa)	Green density (Mg/m ³)	Packing fraction η (%)	DC initial permeability ($\times\mu_0$)
MG150D	490	6.93	88.0	94.9
	686	7.09	90.0	99.1
MG270H	490	6.74	85.7	72.1
	686	6.97	88.5	78.1

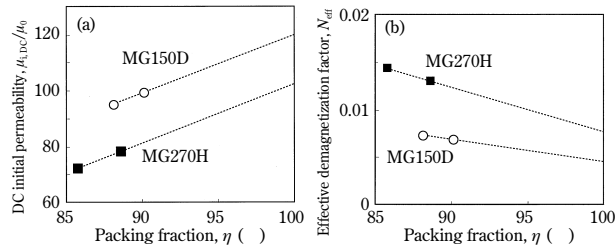


Fig. 3 Packing fraction vs. (a) initial permeability and (b) effective demagnetization factor

powder MG270H over the entire range of measurement frequencies. Since μ_i/μ_0 is approximately constant at frequencies in the vicinity of 10 kHz, the value of μ_i/μ_0 at 10 kHz was regarded as a value for DC initial permeability $\mu_{i,DC}/\mu_0$. **Table 1** shows the thus obtained characteristics of the each test piece derived under this approximation.

The critical frequency f_{CR} defined as the frequency at which the relative initial permeability μ_i/μ_0 is 0.8 times $\mu_{i,DC}/\mu_0$, is 0.6 MHz for both MG150D and MG270H. With iron powder of the conventional particle shape, coarser particle gives larger, $\mu_{i,DC}/\mu_0$, but this is also accompanied by a decrease in f_{CR} .¹⁰⁾ On the contrary, it is a significantly advantageous feature of flaky-shaped powder that it can give an increased initial permeability without being accompanied by a decrease in f_{CR} .

In this connection, it has been confirmed that even when the flaky-shaped MG150D was screened under 45 μm , i.e., smaller than MG270H, a test piece of this powder prepared by the same procedure as described in Chapter 4 still showed a DC relative initial permeability approximately 10% higher than that of MG270H. This result indicates that the higher initial permeability given by the flaky shaped powder is not explained solely by a difference in particle size.

The relationship between the packing fraction η of powder core and DC relative initial permeability $\mu_{i,DC}/\mu_0$ is shown in **Fig. 3(a)**. MG150D gives a higher $\mu_{i,DC}/\mu_0$ than MG270H at the same value of η , and $\mu_{i,DC}/\mu_0$ is close to 100 at η about 90%. This is an improvement of 30–40% in comparison with the conventional reduced iron powder (approximately 80)^{3,4)} and atomized iron powder (approximately 70),⁴⁾ and is at the highest level of iron powder core.

The microstructures of the cross sections of the test pieces compacted at 490 MPa are shown in **Photo 2**.

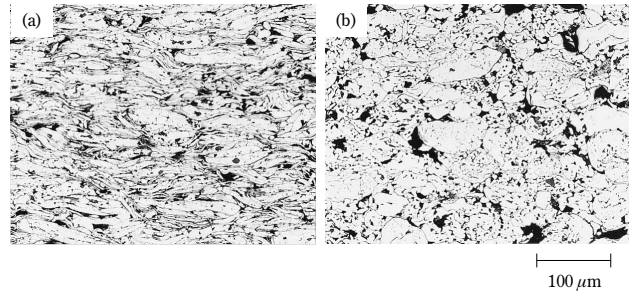


Photo 2 Optical micrograph of the cross section of core samples compacted at 490 MPa: (a) MG150D, (b) MG270H

Here, the horizontal direction in the photographs is the direction of the magnetic field. MG150D, has a layered microstructure in which the plane of the particles aligns to the magnetic field. In contrast, MG270H in Photo 2(b) does not show such a layered microstructure. The similar features were also observed for test pieces prepared at a compaction pressure of 686 MPa. The particle thickness was estimated to be 15 μm for both samples compacted at 490 MPa or 686 MPa from the microstructural observation.

Ozaki et al.⁴⁾ have pointed out that the porous particle structure of reduced iron powder results in a particle deformation after compaction and this gives a higher permeability than that in atomized powder cores through a reduction of the demagnetization effect. Similarly, in the present case, it is considered that particle flattening and alignment proceed even more strongly with flaky-shaped reduced iron powder than with conventional reduced powder, contributing to a further improvement in permeability.

Now we estimate the effective demagnetization factor N_{eff} of the respective test piece using Eq. (2). Intrinsic relative permeability μ_i/μ_0 is estimated as an extrapolation of $\mu_{i,DC}/\mu_0$ in Fig. 3(a) to $\eta = 100\%$.^{4,11)} The values obtained are 120 for MG150D, and 102 for MG270H. The calculated N_{eff} is shown in Fig. 3(b) as a function on η . These results confirm that the values of N_{eff} for MG150D are approximately 1/2 those for MG270H.

5.2 Core Loss

Figure 4 shows core loss P_{cv} at a magnetic flux density of 50 mT as a function of frequency f for the test pieces compacted at 686 MPa. The values of P_{cv} are lower with MG150D than with MG270H over the entire range of frequencies. In other words, it is suggested that the improved permeability achieved by particle shape modification is not accompanied by an increase in core loss.

Core loss P_{cv} is given as a sum of two components, hysteresis loss P_h and eddy current loss P_e .¹²⁾ Of these two components, P_e is proportional to the square of f , whereas P_h is proportional to f . Accordingly, using the constants A and B defined by $P_h = Af$ and $P_e = Bf^2$,

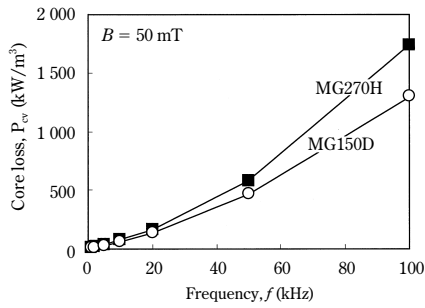


Fig. 4 Frequency dependence of core loss for samples compacted at 686 MPa

respectively. The value P_{cv}/f is given as

$$P_{cv}/f = A + Bf \dots \dots \dots (3)$$

The residual loss of the third component has been ignored in the following discussion. In fact, as shown in Fig. 5, P_{cv}/f vs f plot gives a linear relationship as predicted from Eq. 3. P_h and P_e can be calculated if the constants A and B are obtained by a least square fitting calculation of his linear relationship expressed by Eq. (3). Figure 6 shows P_h and P_e at a frequency of 100 kHz. Comparing MG150D with MG270H, the component P_e shows a significant difference. From this finding, it can be understood that the difference in core loss P_{cv} as seen in Fig. 4, is mainly attributable to a difference in the eddy current loss.

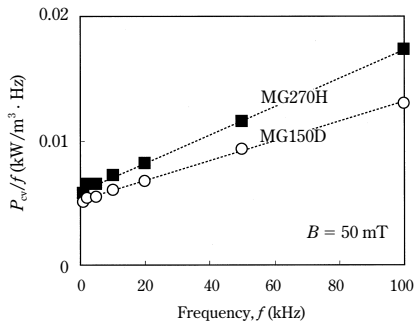


Fig. 5 Frequency dependence of P_{cv}/f based on the core loss data shown in Fig. 4

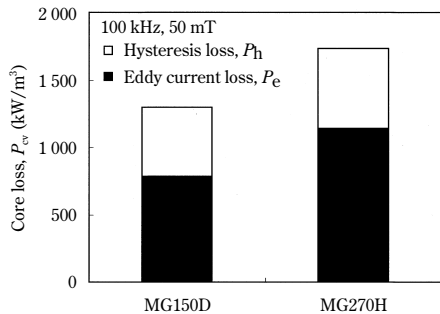


Fig. 6 Eddy current losses and hysteresis losses derived from the relationship of P_{cv}/f vs. f in Fig. 5

5.3 Relationship between Microstructure and Magnetic Properties

Eddy current loss in powder cores consists of two components, one component comes from current flow within the individual iron powder particles (intraparticle eddy current) and the other component resulting from current flow across particles (interparticle eddy current).¹¹⁾ Of the two components, the interparticle eddy current can be suppressed by applying electrical insulation between the particles. In order to investigate the contribution of intergrain eddy current in MG150D powder cores, test pieces with different epoxy resin were prepared through the same process as described in Chapter 4. Figure 7 shows the core loss as a function of the epoxy resin content. In all cases, the compaction pressure was 686 MPa, and the core loss measurement frequency and magnetic flux density were 100 kHz and 50 mT, respectively. Core loss decreases as the resin content increases until 1% and beyond this content, it becomes substantially constant. It is considered that in a range of 1% or more interparticle insulation is maintained in such a condition that the contribution of interparticle eddy current to the total loss becomes sufficiently small as compared with that of intraparticle eddy current. Therefore, in the following discussion, we assume that the intraparticle current dominate the eddy current loss for test pieces with 1% epoxy resin content shown in Fig. 6.

When an AC magnetic field with magnetic flux density B (T) and frequency f (Hz) is applied the eddy current loss P_e (W/m³) generated in an object with a specific resistivity ρ (Ω m) is expressed by Eq. (4).¹³⁾

$$P_e = (\pi a f B)^2 / k \rho \dots \dots \dots (4)$$

Here, k is a constant which is dependent on the shape of the object. The values of k are 20 and 6 for a sphere with a diameter of a (m) and a sheet with a thickness of a (m) under a parallel magnetic field, respectively. Although this expression was derived on for a single object, Fujiwara et al.¹⁴⁾ calculated the eddy current losses for an

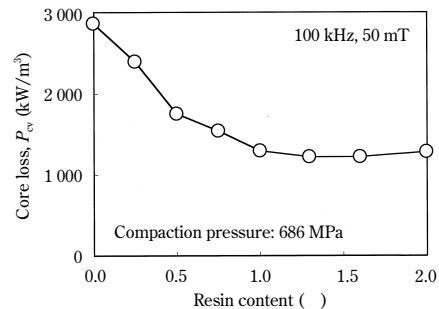


Fig. 7 Relationship between core loss and resin content for flaky-shaped powder based core samples

alloy powder core using a similar model on an assumption that magnetic particles in the alloy are regarded as a sphere with a diameter equivalent to the average particle size. Since comparison of the calculated values with measured one showed a good agreement, it is indicated that it is possible to apply the model expressed by Eq. (4) to a multi-particle system such as a powder core.

Because the average particle thickness of MG150D is $15\ \mu\text{m}$, as described in section 5.1, the particles are assumed to comprise a sheet of this thickness. According to Eq. (4), in order to obtain the same P_e for a spherical particle as that for a sheet-shaped particle of this thickness of $15\ \mu\text{m}$, the diameter of the sphere should be $27\ \mu\text{m}$, which corresponds to approximately 1/3 of the average diameter of the MG270H iron powder. Thus, it is suggested that the reason why eddy current loss is smaller in MG150D, as shown in Fig. 6, is because the eddy current is suppressed by the layered microstructure wherein the flaky-shaped particles are aligned in the direction of the magnetic field.

For conventional reduced powder, if the particle size is decreased in order to suppress the eddy current, $\mu_{i,DC}/\mu_0$ decrease.¹⁰⁾ In fact a MG270H based powder screened under $45\ \mu\text{m}$ gives a core with screened under showed $\mu_{i,DC}/\mu_0$ approximately 10% lower in comparison the standard size MG270H. Thus in the case of the particle size $27\ \mu\text{m}$, the $\mu_{i,DC}/\mu_0$ value would show an even lower value. In contrast, particle shape modification is an advantageous technology to satisfy the requirements of both higher initial permeability and reduced eddy current loss, which are the mutually incompatible with the conventional type of iron powder.

Based on Eq. (4), a reverse calculation of the particle thickness of MG150D is carried out using the value of P_e separated from the observed loss data in the previous section. Here, we assume that $k = 6$, because the flake-shaped particles approximated as a sheet in shape, as described previously. Taking the value of $784\ \text{kW/m}^3$ as the eddy current loss, P_e at $f = 100\ \text{kHz}$ and $B = 50\ \text{mT}$, and the specific resistance of pure iron ($8.9 \times 10^{-8}\ \Omega\text{m}$) as the ρ value the particle thickness a can be calculated as $41\ \mu\text{m}$. This calculated value is approximately 3 times larger than the measured average particle ($15\ \mu\text{m}$) obtained from the microstructure.

There are some possible reasons for the discrepancy such as an imperfection of the inter-particle insulation, the finite particle dimension along the layered structure, or deformation of the layered structure through the imperfect particle alignment. The flow rate of MG150D and MG270H are $38.7\text{s}/50\text{g}$ and $18.5\text{s}/50\text{g}$, respectively. For the flaky-shaped powder, this low flowability would cause an inhomogeneous inter-particle insulation and a misalignment through the compaction process. Therefore, the actual system is not a perfectly layered structure but an intermediate arrangement between a stack of

plates and a compact of round particles. Then, the magnetic properties would be further enhanced through the improvement of the particle insulation and alignment.

Finally, the optimized property of a MG150D core is evaluated. The ideal microstructure of a MG150D core is assumed to be a lamination of $15\ \mu\text{m}$ -thick layers. Applying Eq. (4) with $k = 6$, we can estimate P_e at $f = 100\ \text{kHz}$ and $B = 50\ \text{mT}$ as $104\ \text{kW/m}^3$. If P_h is kept as shown in Fig. 6, the total loss P_{cv} will be $620\ \text{kW/m}^3$, which is about 1/2 times the present value.

6 Conclusion

- (1) A new flaky-shaped iron powder MG150D has been developed. The developed iron powder improves remarkably the initial permeability of powder cores in comparison with the conventional reduced iron powder.
- (2) DC relative initial permeability of the powder core made from MG150D is close to 100. This is at the highest level of iron powder cores.
- (3) The effective demagnetization factor of powder cores made from MG150D is approximately 1/2 of that of cores made from the conventional reduced iron powder, which is not flake-shaped. The low effective demagnetization contributes to improved permeability.
- (4) The improvement in permeability arising from flake-shape is not accompanied by a deterioration in core loss. It is presumed that the layered structure in the powder core, in which the planes of the powder particles are aligned along the field direction, has the effect of suppressing eddy current.

References

- 1) K. Tange: *Nikko Material*, **2**(1984), 16
- 2) T. Sawa, Y. Hirose, and K. Inomata: *Toshiba Review*, **39** (1984), 735
- 3) Y. Ozaki and M. Fujinaga: *Kawasaki Steel Technical Report*, (2000)42, 30
- 4) Y. Ozaki, M. Ueta, and M. Fujinaga: *J. of Jpn. Soc. of Powder*, **47**(2000), 711
- 5) T. Nishida, T. Kikuchi, S. Sato, and T. Ichiyama: *J. of Jpn. Inst. of Metals*, **42**(1978), 593
- 6) H. Mitani, A. Hanaki, H. Ieguchi, and Y. Seki: *Kobe Steel Engineering Reports*, **48**(1998), 25
- 7) S. Chikazumi: "Physics of Ferromagnetic Materials", (1978), 13, [Shokabo]
- 8) F. Ollendorf: *Arch. Elektrotechn.*, **25**(1931), 436
- 9) National Astronomical Observatory: "Chronological Scientific Tables 2000", (2000), 482, [Maruzen]
- 10) P. Jansson: Proc. of the 1999 Int. Conf. on Powder Metallurgy & Particular Materials, (1999)Part 8, 3
- 11) S. Takajo: *Bull. of Jpn. Inst. of Metals*, **29**(1990)3, 141
- 12) T. Saito: *Electronic Furnace Steel*, **69**(1998), 181
- 13) R.M. Bozorth: "Ferromagnetism", (1993), 778, [IEEE Press]
- 14) T. Fujiwara and M. Ishii: *Tokin Technical Review*, **27**(2000), 14